Article

Photocatalytic Degradation of Pharmaceutical Trimethoprim in Aqueous Solution over Nanostructured TiO$_2$ Film Irradiated with Simulated Solar Radiation

Davor Ljubas [1,*] , Hrvoje Juretić [1,*], Alan Badrov [2], Martina Biošić [2] and Sandra Babić [2]

1 Faculty of Mechanical Engineering and Naval Architecture, University of Zagreb, Ivana Lučića 5, 10000 Zagreb, Croatia
2 Faculty of Chemical Engineering and Technology, University of Zagreb, Trg Marka Marulića 19, 10000 Zagreb, Croatia; abadrov@fkit.hr (A.B.); sbabic@fkit.hr (S.B.)
* Correspondence: davor.ljubas@fsb.hr (D.L.); hrvoje.juretic@fsb.hr (H.J.)

Abstract: Pharmaceuticals are characterized by a wide range of physical, chemical, and biological properties and functionalities that contribute to their inherent complexity as compounds. Unfortunately, human carelessness during the production, use, and disposal of these compounds results in their presence in the environment. This study utilized a nanostructured TiO$_2$ film on a glass ring at the bottom of a reactor and simulated a solar radiation lamp as the radiation source for both photocatalytic and photolytic experiments, with the aim of unraveling the mechanism behind the degradation of trimethoprim (TMP), a pharmaceutical compound. This approach provides a novel perspective on the role of TiO$_2$ in the degradation of pharmaceuticals and could pave the way for more efficient and sustainable wastewater treatment methods. Scavenger studies were carried out using isopropanol, ammonium oxalate, and triethanolamine to examine the photocatalytic mechanism. Isopropanol and triethanolamine were found to impede the photocatalytic degradation of TMP, highlighting the significance of hydroxyl radicals and positive holes in the degradation process, while no inhibition was observed in the presence of ammonium oxalate. The complete degradation of TMP through photocatalysis under simulated solar radiation was observed in ultra-pure water in fewer than 3 h, as indicated by the results. Our findings suggest that utilizing natural solar radiation as a source of UV-A radiation in reactor configurations based on this approach holds promise for cost-effective pharmaceutical degradation treatment in wastewater treatment plants. The practical potential of this approach is supported by the results obtained under simulated solar radiation with an irradiation intensity in the UV-A region of 33 ± 2 W/m^2.

Keywords: trimethoprim; photolysis; photocatalysis; simulated solar radiation; degradation mechanisms; degradation products; TiO$_2$

1. Introduction

Ground and surface waters are continually contaminated by various types of inorganic and organic pollutants. These include a group of substances labelled as micropollutants, consisting of a growing array of substances, such as endocrine disruptors, pharmaceuticals, personal care products, hormones, industrial chemicals, flame retardants, pesticides, and various other compounds [1]. Most compounds in this group have no guidelines, norms, or rules limiting their discharge into the environment. Numerous investigations have demonstrated the presence of certain groups of micropollutants in the environment. Concerns over this issue are reflected in European legislation (Water Framework Directive, Priority Substances, Watch List, Watch List Candidates). The list of organic micropollutants also includes substances used as pharmaceuticals for human and animal use such as synthetic hormones, personal care products, etc. [2].

Micropollutants are typically found in low concentrations in the range of several nanograms per liter to several micrograms per liter [3]. The presence of micropollutants in low concentrations and their diverse natures pose significant challenges for detection, analysis, and water treatment processes [4]. The existing technologies and infrastructure for preparing drinking water and treating wastewater have reached their limits in ensuring adequate water quality to meet human and ecological needs. Wastewater treatment is being increasingly developed, in part due to progress in analytical methods but also thanks to new medical findings on the harmfulness of certain substances that circulate through wastewater and end up in sources of drinking water [2,5]. Although some micropollutants can be removed or degraded by conventional biological wastewater treatment plants (WWTP), a significant number of them are resistant to existing and common processing methods [6]. Among the substances used in human practice to eliminate other microorganisms and organisms potentially harmful to humans and animals, two groups of substances are particularly important: pesticides and pharmaceuticals [7,8]. This study focuses on the challenges associated with pharmaceuticals. Pharmaceuticals are considered complex compounds due to their diverse physical, chemical, and biological properties, and functionalities. Even though they are present in low concentrations (ng/L to µg/L) in aquatic environments, their continuous release into the environment can lead to harmful effects on non-target organisms [8]. Therefore, it is essential to prevent their release into the environment, particularly from wastewater treatment plants, where conventional treatment technologies are often ineffective at removing these compounds [9]. Alternative strategies for wastewater treatment that can successfully remove pharmaceuticals should be explored and adopted urgently.

TMP (2,4-diamino-5(3′,4′,5′-trimetoxybenzylpyrimidine) is an antibiotic that is commonly prescribed in both veterinary and human medicine to treat a variety of infections, including those affecting the respiratory, urinary, and gastrointestinal tracts [10]. It is considered to be one of the most frequently used antibiotics. Approximately 20% of TMP is metabolized, mainly in the liver, while the remainder is excreted unchanged in the urine and can potentially reach the environment through incomplete removal in a WWT plant. According to the authors' previous research, TMP exhibits resistance to biodegradation and hydrolysis, but its environmental concentration can be decreased by slow degradation in favorable conditions through solar radiation [10]. TMP has been included in the watchlist by the European Union since 2020 ((EU) 2018/840) to improve knowledge about the occurrence and spread of antimicrobials in the environment. The observation of TMP in elevated concentrations in wastewater has raised concerns related to the possibility of the occurrence of antibiotic-resistant bacteria [11,12]. This can lead to the development of antibiotic-resistant genes in natural water bodies and an increase in the occurrence of infections [13]. In article [14], a group of fourteen high-risk drugs was observed in hospital wastewaters, all of which have a hazard ratio greater than 10; TMP is included among them.

Because of its frequent use and the fact that it is not effectively eliminated in wastewater treatment plants, TMP is frequently detected in wastewater effluents and surface waters. This highlights the need to remove it from the wastewater prior to its release into the environment. Several methods have been suggested for the degradation of trimethoprim, which include advanced oxidation processes (AOPs) like ozonation [15–19], membrane processes such as nanofiltration and reverse osmosis [20,21], sonochemical processes [22], combined treatments [23], and adsorption processes [24,25].

Over the past few decades, nanotechnology has rapidly emerged as a growing knowledge-based economy sector, primarily due to the unique physicochemical properties of nanomaterials. This technology has been widely encouraged because it has the potential to transform particles of metal, metal oxides, and other materials, often hybrid, into a new nano-form, which is smaller than 100 nm. Various types of nanomaterials, including magnetic nanoparticles, semiconductors, double hydroxide layers, ion exchange resins, alumosilicates, and graphene-based nanocomposites, have been utilized in water treatment technologies [26–30].

Out of the aforementioned nanomaterials, the authors opted to utilize a photocatalytic material in the form of a nanostructured TiO_2 film, adhered to a glass substrate. The use of such photocatalytic material to degrade organic micropollutants in water is classified as an AOP. TiO_2 has been the catalyst most used in research exploring the photocatalytic degradation of pharmaceuticals [31–34].

In many photocatalytic studies, TiO_2 has been used in a suspended form for degrading organic pollutants. However, the immobilization of TiO_2 onto a substrate has been shown to result in lower efficiency due to a reduced number of active sites for generating oxidizing $^{\bullet}OH$ radicals or oxidizing positive holes (h^+), compared to suspended TiO_2 catalysts [35,36].

However, the high cost and time required for the catalyst recovery and separation in the slurry system render it impractical for use in real-world applications. To address this, the authors concluded that a fixed bed approach, utilizing deposited photocatalytic films, would be more practical [37–39]. The authors of this study examined the degradation of TMP through photocatalysis using a specialized nanostructured film placed on borosilicate glass with a distinct shape and located at the base of a reactor that is exposed to radiation. During the nanostructured film preparation, the same procedure, as in [40], was followed, including the addition of PEG (polyethylene glycol, M_r = 5000–7000, as an organic/polymer additive for increasing the surface roughness and, therewith, increasing the photocatalytic activity of the film) and calcination at 550 °C, which results in the formation of the photocatalytic film that consists only of anatase TiO_2 and shows granular microstructures with almost monodispersed spherical particles. The film was characterized by the following methods: XRD, AFM, FTIR, and Micro-Raman spectroscopy; and their results are also shown in references [39,40]. The lamp used in the experiments was a sun simulator lamp, and the authors aimed to determine the reliability of using cheap natural solar radiation as the only source of energy required for the complete degradation of pharmaceuticals, such as TMP, in wastewater streams before their release into the environment.

2. Materials and Methods

2.1. Chemicals

The high purity (>98%) analytical standard of trimethoprim (TMP) (2,4-diamino-5(3′,4′,5′-trimetoxybenzylpyrimidine) (CAS no. 738-70-5) was supplied from Sigma-Aldrich (St. Louis, MO, USA). Triethanolamine (CAS no. 102-71-6) was obtained from Carlo Erba Reagents (Milan, Italy), while ammonium oxalate (CAS no. 6009-70-7) was purchased by Kemika (Zagreb, Croatia). Isopropanol (CAS no. 67-63-0) was supplied by Fisher Chemicals (Loughborough, UK), and HPLC grade acetonitrile (J. T. Baker, Deventer, The Netherlands) and formic acid (Lachner, Zagreb, Croatia) were also used.

The chemicals used for the preparation of the nanostructured photocatalytic film included titanium (IV) isopropoxide (TIP), i-propanol (PROH), nitric acid (NA), acetylacetone (AA), and PEG (polyethylene glycol). Ultra-pure water was prepared using the Millipore Simplicity UV system (Millipore Corporation, Billerica, MA, USA).

### 2.2. Preparation of Nanostructured Photocatalytic Film

A detailed description of the sol-gel process used to create a nanostructured sol-gel TiO_2 film, in the crystal form of anatase, can be found in [39,40]. The film was deposited onto a borosilicate glass ring using a range of chemicals, including titanium (IV) isopropoxide ($Ti(C_3H_7O)_4$)-TIP, i-propanol (C_3H_7OH)-PROH, nitric acid (HNO_3)-NA, acetylacetone ($CH_3(CO)CH_2(CO)CH_3$)-AA and PEG ($HO(C_2H_4O)nH$). These chemicals were utilized as a Ti precursor, solvent, catalyst, for peptization, and organic/polymer additive, respectively. The TIP:PROH:AA:NA molar ratio was carefully controlled and was set to 1:39:0.71:0.017. This resulted in the formation of a high-quality film that was perfectly suited to our research needs.

2.3. Photolytic/Photocatalytic Experiments

A simulated solar radiation lamp (model SOL 500 by Dr. Hönle AG, Gilching, Germany) was used as the source of radiation for both photolytic and photocatalytic experiments. The irradiation spectrum of the lamp is given in Figure S1 in the Supplementary Materials.

During the photolytic experiments, a reactor filled with 100 mL of the model TMP solution (10 mg/L, $25 \pm 0.2\ °C$) was solely exposed to the lamp radiation.

In contrast, during the photocatalytic experiments, a glass ring with a deposited photocatalyst was placed at the bottom of the same reactor (Figure 1). The dimensions of the glass ring were $D_{external}$ = 90 mm, $D_{internal}$ = 30 mm, and height = 5 mm. The UV-A irradiation intensity in the reactor was adjusted to $33 \pm 2\ W/m^2$, with global irradiation set to $975 \pm 6\ W/m^2$, and was regularly monitored to simulate the near maximum natural noon solar irradiation for the region of Zagreb, Croatia. Adjustment of the irradiation intensity was achieved by positioning the lamp 15 cm above the reactor. Global irradiation from the solar simulator lamp was measured using a pyranometer model CMP11 (Kipp & Zonen Co., Delft, The Netherlands), while UV-A irradiation was measured using a radiometer equipped with a UV-A sensor in the 315–400 nm range, model RM 21 (Opsytec Dr. Gröbel Co., Ettlingen, Germany).
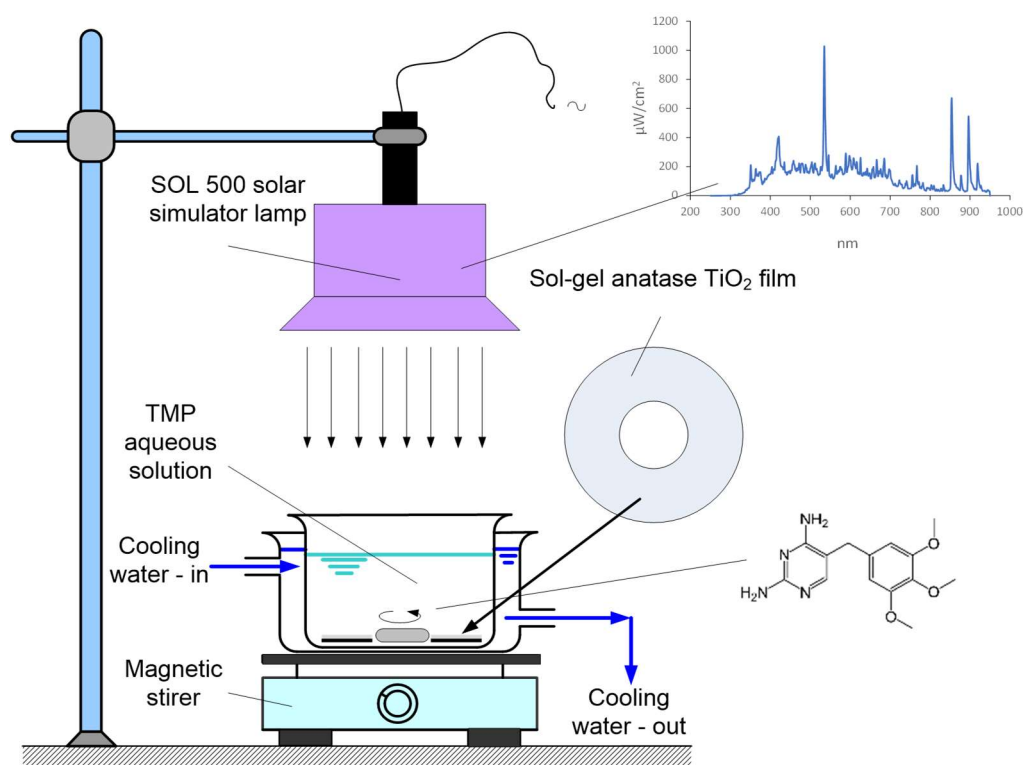
Figure 1. Schematic representation of the experimental set-up.

The photocatalytic mechanism was investigated through scavenger studies utilizing isopropanol, ammonium oxalate, and triethanolamine as scavengers for hydroxyl radicals, superoxide radicals, and positive holes, respectively [41,42]. The experimental study consisted of the following:

- evaluation of adsorption processes (stirring "in the dark");
- photolytic degradation experiments (irradiation without TiO_2 ring);
- photocatalytic degradation experiments (irradiation with the TiO_2 film at the bottom of the reactor);
- photocatalytic degradation experiments carried out using different scavengers.

Typically, in photocatalytic degradation processes, a continuous stream of oxygen or air is supplied to the solution through bubbling. However, in this experiment, such a supply was not required because the stirring created a whirlpool in the solution, which allowed for sufficient oxygen uptake to approach the maximum saturation level in the solution.

Finally, the total energy consumption for the photodegradation process of TMP was followed by a power meter, the model Voltcraft Energy Check 3000 (Conrad Co., Wernberg-Köblitz, Germany). The projection of energy savings is based on the assumption of the same irradiation intensity in the experimental region of Zagreb, Croatia, during the period from 10.30 a.m. to 1.30 p.m., when the solar radiation intensity is at its highest.

Samples were periodically withdrawn from the reaction mixture and analyzed for the residual amount of TMP using HPLC-PDA and HPLC-MS/MS.

All experiments were made in triplicates and the values shown in diagrams are the average arithmetic values of the three experiments, with all experimental results obtained within ±5% from the average value that is shown in diagrams.

2.4. Apparatus and Analytical Procedures

The degradation rates of TMP during photolytic and photocatalytic experiments were determined using a Waters 2795 Alliance high performance liquid chromatography (HPLC) system coupled with a 2996 photodiode array (PDA) detector. The Kinetex C18 chromatographic column (Phenomenex, 150 mm × 4.6 mm, 5 mm, 100 Å) was used for chromatographic separation. Eluent A consisted of MilliQ water containing 0.1% formic acid, while eluent B was acetonitrile containing 0.1% formic acid. The analysis was carried out with isocratic elution and mobile phase composition A:B = 90:10 (v/v). The flow rate was maintained at 1.0 mL/min throughout the analysis with an injection volume of 20 μL. TMP was detected at the wavelength of 273.8 nm.

Samples from photolytic and photocatalytic degradation experiments analyzed using an Agilent Series 1200 HPLC system (Santa Clara, CA, USA) coupled with an Agilent 6410 triple-quadrupole mass spectrometer equipped with an ESI interface (Santa Clara, CA, USA). Chromatographic separation was performed on a Synergy Hydro-RP Fusion embedded column (100 mm × 2.0 mm, particle size 2.5 μm) (Phenomenex, Torrance, CA, USA) using mobile phase, comprising MilliQ water with 0.1% formic acid as eluent A and acetonitrile with 0.1% formic acid as eluent B. The elution gradient started with 90% of eluent A, which was kept constant for the next 5 min. In the next 10 min, the proportion of eluent was decreased to 70% and was kept for 7 min. In the next 3 min, the proportion of eluent A decreased to 5% and remained for the next 8 min. In the next 1 min, the proportion of eluant A was returned to the initial value (90%) and kept for 10 min. The flow rate of 0.2 mL/min was maintained throughout the analysis. An injection volume of 5 μL was used in all analyses. The analyses were conducted in positive ion mode under the following conditions: drying gas temperature 350 °C, drying gas flow 11 L/min, capillary voltage 4.0 kV, and a nebulizer pressure of 35 psi. Instrument control and data acquisition and evaluation were performed with Agilent MassHunter 2003–2007 Data Acquisition for Triple Quad software version B.01.04 (B84) (Santa Clara, CA, USA).

Total organic carbon (TOC) analyses were performed using a TOC analyzer, type TOC-VCPH (Shimadzu, Kyoto, Japan) via the non-purgeable organic carbon (NPOC) method.

The global simulated solar radiation was measured using a pyranometer (Kipp & Zonen Co., Delft, The Netherlands), model CMP11, while the UV-A radiation was measured using an RM 21 radiometer equipped with an UV-A Opsytec sensor manufactured by Dr. Gröbel (Ettlingen, Germany).
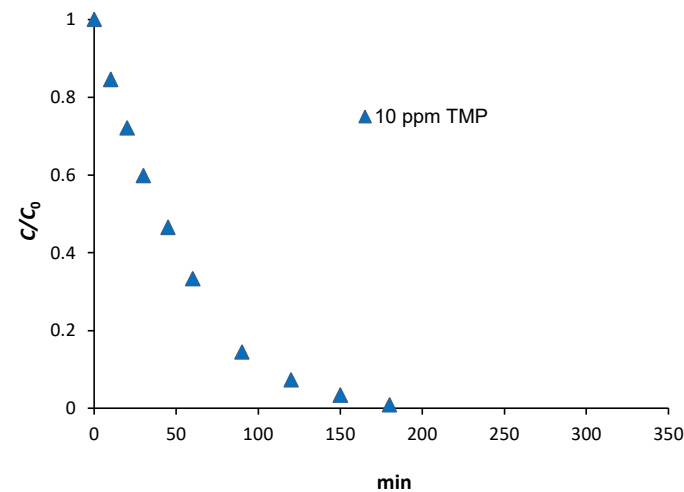
3. Results

3.1. Photolysis and Photocatalysis

The photolytic degradation process of TMP is presented in Figure 2. The graph indicates that the complete degradation of TMP requires at least 5 h of irradiation with simulated solar radiation. However, when the photocatalytic film on the bottom of the

reactor is introduced, the time required for complete degradation is reduced to fewer than 3 h, as shown in Figure 3.
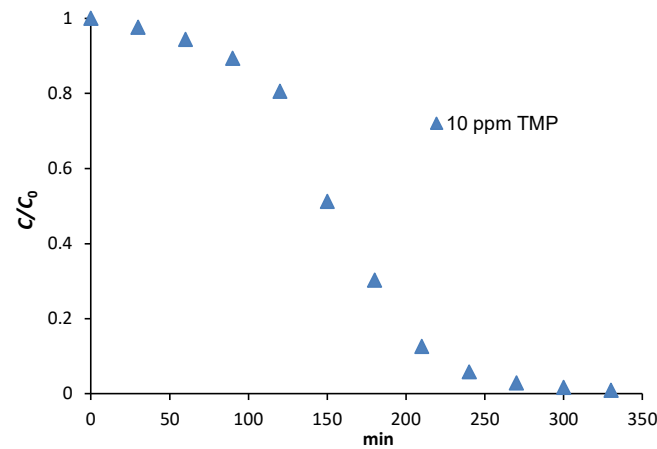

Figure 2. Photolytic degradation of TMP.

Figure 3. Photocatalytic degradation of TMP.

The results of our study confirm that TMP can be effectively degraded through photolysis, as previously stated in the study [10]. Moreover, it has been reported that TMP is highly resistant to hydrolysis (with a half-life of 1 year at 25 °C) and biodegradation (not susceptible to biodegradation). Therefore, in natural water environments, photolysis is the only effective process for eliminating TMP residuals, reducing its potential harmful impact on both humans and the environment [14].

The photolytic degradation of TMP did not follow first-order kinetics. As depicted in Figure 2, there was only a slight decrease in TMP concentration during the initial 100 min, followed by a much faster degradation rate. This degradation profile suggests that there may be different degradation mechanisms present, with the initial degradation being slow due to the direct radiation exposure of the TMP solution. In the second part, a faster degradation occurs due to the formation of photoreactive degradation products that initiate autocatalytic decomposition [43]. To confirm this, the formation of TMP degradation products was monitored by observing the appearance of new chromatographic peaks during the photolysis experiments. It was observed that, as the TMP peak on the chromatograms decreased, two new peaks—degradation products (DP) 1 and 2—appeared and increased (Figure 4). As the experiment progressed, the peaks of DPs decreased, and one of them disappeared entirely up to 300 min, indicating that the degradation products

formed from TMP are also photolytically degraded. As shown in Figure 4, the formation of TMP photodegradation products occurs in the second part of faster degradation of TMP, possibly due to the critical amount of photodegradation products formed, which then act photocatalytically.
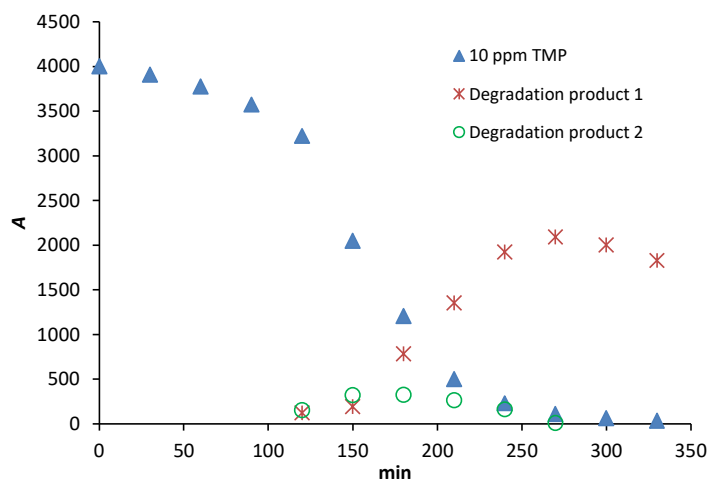
Figure 4. Degradation/formation profiles of TMP and its degradation products.

The formation and degradation of DP1 and DP2 (Figure 4 and Figure S2 in the Supplementary Material) was monitored through the increase/decrease of the chromatographic peak areas (*A*), which are proportional to their concentrations. Because there are no DP1 and DP2 standards it was not possible to convert the chromatographic peak areas into the corresponding concentrations.

In order to elucidate the structures of the detected products of photolytic degradation, as well as to detect and elucidate the structures of the photocatalytic degradation products, HPLC-MS/MS analysis was performed. The tentative structures of TMP degradation products (Table 1) were proposed based on their retention times, *m*/*z*-values, and fragmentation patterns, obtained through the HPLC-MS/MS analysis. Mass spectra of TMP and its degradation products are shown in the Supplementary Material, Figure S3. In total, five degradation products were identified. All five were detected in the reaction solution from the photocatalytic experiments, while only DP1 and DP2 were identified during photolytic degradation. The identified DP1 and DP are the same degradation products identified by Biošić et al. [10] as photolytic degradation products under environmentally relevant conditions.
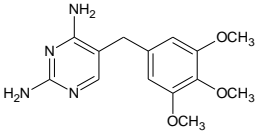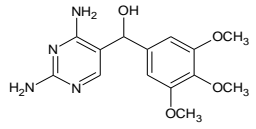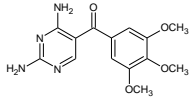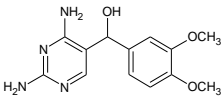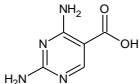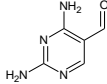
### 3.2. Mechanism of Photocatalytic Degradation

Experiments were also performed to gain a detailed understanding of the degradation mechanism of TMP during photocatalytic degradation. To achieve this, three different series of experiments were conducted with the lamp switched on:

(i)   experiments with the addition of isopropanol to verify the role and action of hydroxyl radicals ($^{\bullet}OH$);

(ii) experiments with the addition of ammonium oxalate to verify the role and action of superoxide radicals ($^{\bullet}O_2^-$);

(iii) experiments with the addition of triethanolamine to verify the role and action of positive holes (h^+).

It was assumed that isopropanol acts as a scavenger of $^{\bullet}OH$ radicals, ammonium oxalate acts as a scavenger of superoxide radicals, and triethanolamine acts as a positive hole (h^+) scavenger [41,42]. The influence of these radical scavengers is shown in Figures 5–7. Additionally, experiments were conducted in the dark, with the lamp switched off, to confirm that the adsorption process of TMP on the film was negligible.

Table 1. Tentative structures of photolytic and photocatalytic degradation products of TMP.

Compound	Chemical Formula	Chemical Structure
TMP [M+H]$^+$ *m/z* 261 *m/z* 230 *m/z* 123 *m/z* 109	$C_{14}H_{19}N_4O_3$ $C_{12}H_{13}N_4O_3$ $C_{12}H_{14}N_4O$ $C_5H_7N_4$ $C_4H_5N_4$	
DP-1 [M+H]$^+$ *m/z* 289 *m/z* 259 *m/z* 243	$C_{14}H_{19}N_4O_4$ $C_{14}H_{17}N_4O_3$ $C_{13}H_{15}N_4O_2$ $C_{12}H_{11}N_4O_2$	
DP-2 [M+H]$^+$ *m/z* 289 *m/z* 137	$C_{14}H_{17}N_4O_4$ $C_{13}H_{13}N_4O_4$ $C_5H_5N_4O$	
DP-3 [M+H]$^+$ *m/z* 261 *m/z* 246 *m/z* 216	$C_{13}H_{17}N_4O_3$ $C_{13}H_{17}N_4O_2$ $C_{13}H_{16}N_3O_2$ $C_{12}H_{14}N_3O$	
DP-4 [M+H]$^+$ *m/z* 137	$C_5H_7N_4O_2$ $C_5H_5N_4O$	
DP-5 [M+H]$^+$ *m/z* 96	$C_5H_7N_4O$ $C_4H_6N_3$	
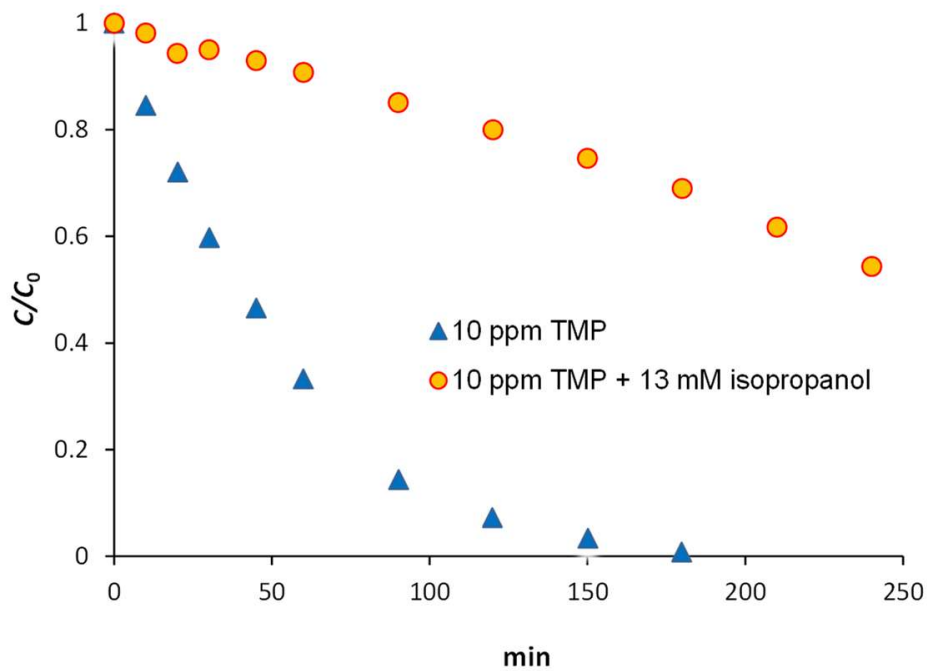
Figure 5. Degradation of TMP with and without isopropanol.
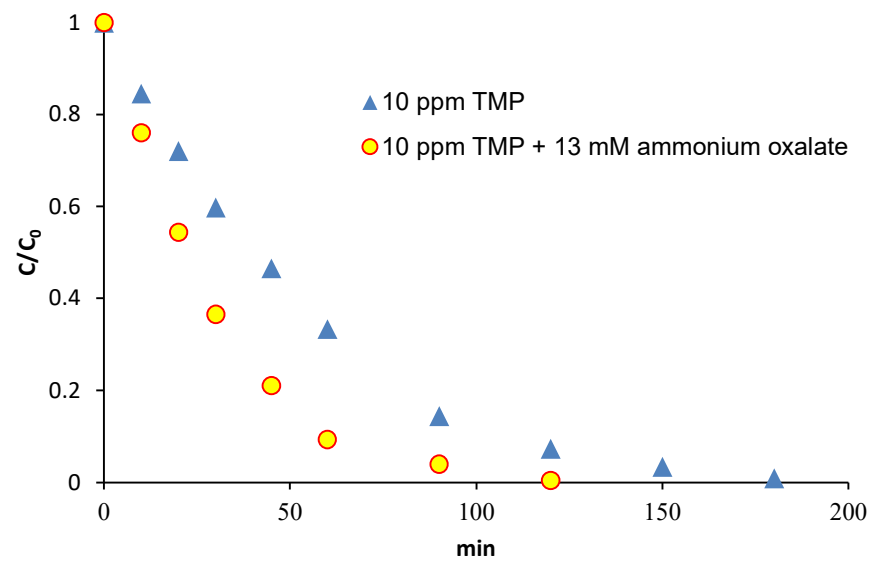
Figure 6. Degradation of TMP with and without ammonium oxalate.
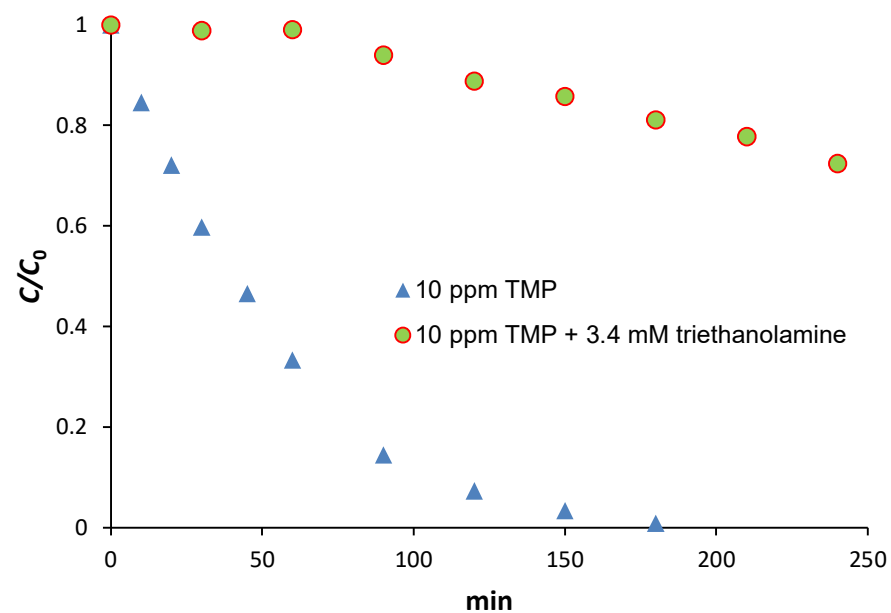
Figure 7. Degradation of TMP with and without triethanolamine.

In Figure 5, a significant scavenging effect of isopropanol was observed, as shown by the high C/C_0 ratio. The C/C_0 ratio represents the ratio of the current chromatographic peak area of TMP (which changes over time) to the initial peak area, obtained by the HPLC system with PDA detector, with an initial concentration of 10 mg/L. This ratio is also shown in other Figures 5–7.

When ammonium oxalate was added (Figure 6), the degradation mechanism changed, resulting in an accelerated rate of degradation. It seems that superoxide radicals are not the mechanism of TMP degradation. It is possible that the pH increase caused by the addition of ammonium oxalate to the solution led to an increase in the degradation rate, as supported by a 33% increase in the degradation rate constant.

Figure 7 shows that the addition of triethanolamine led to a significantly slower reaction, suggesting a significant dependence of the degradation mechanism on the positive holes.

According to the data shown in Figures 5–7, it can be concluded that it seems the main mechanisms of the TMP degradation are the acting of $^\bullet$OH radicals and oxidizing

positive holes (h^+). The process of their generation on the photocatalytic film that consists of anatase TiO_2 is irradiation with wavelengths below 387.5 nm (UV-A region), i.e., with energy higher than 3.20 eV (bandgap of the anatase TiO_2). Solar radiation can be used for this process, although the efficiency in this case is relatively low—only approximately 3–5% of the global solar radiation consists of the wavelengths in the UV-A region, but it is still enough for use for the oxidation of the organic matter in water. We conducted experiments simulating the most favorable situation, which is solar radiation at the time of the day when it is most intense—at approximately noon. In other parts of the day, the radiation is less intense and the organic matter degradation would be less efficient.

In this study, a first-order model was assumed for the photocatalytic degradation of TMP with TiO_2, consistent with previous findings [4,37,44]. The results of the trendline analysis, with and without scavengers, revealed high R^2 values, indicating a good fit of the data to the model. Table 2 summarizes the values of the degradation rate constant (k_r) and half-life ($t_{1/2}$) obtained from the trendline analysis, demonstrating the significant effect of scavengers on the degradation process.

Table 2. Photocatalytic degradation rate constant, R^2 and half-life.

	Trendline and R^2	k_r, min^{-1}	$t_{1/2}$, min
TMP 10 ppm	y = −0.0253x + 0.2271 R^2 = 0.9822	0.0253	27.4
TMP 10 ppm + 13 mM isopropanol	y = −0.0023x + 0.018 R^2 = 0.9649	0.0023	301.4
TMP 10 ppm + 13 mM ammonium oxalate	y = −0.0374x + 0.0717 R^2 = 0.9928	0.0374	18.53
TMP 10 ppm + 3.4 mM triethanolamine	y = −0.0013x + 0.0328 R^2 = 0.9697	0.0013	533.2

3.3. Dependence of Degradation Rate of TMP on pH Value

The natural pH of the 10 ppm TMP solution in ultra-pure water was 5.59 at 25 °C. Figure 8 illustrates the relationship between the degradation rate and pH values for photocatalytic degradation. The pH values chosen for the experiments are representative of those found in environmental waters.
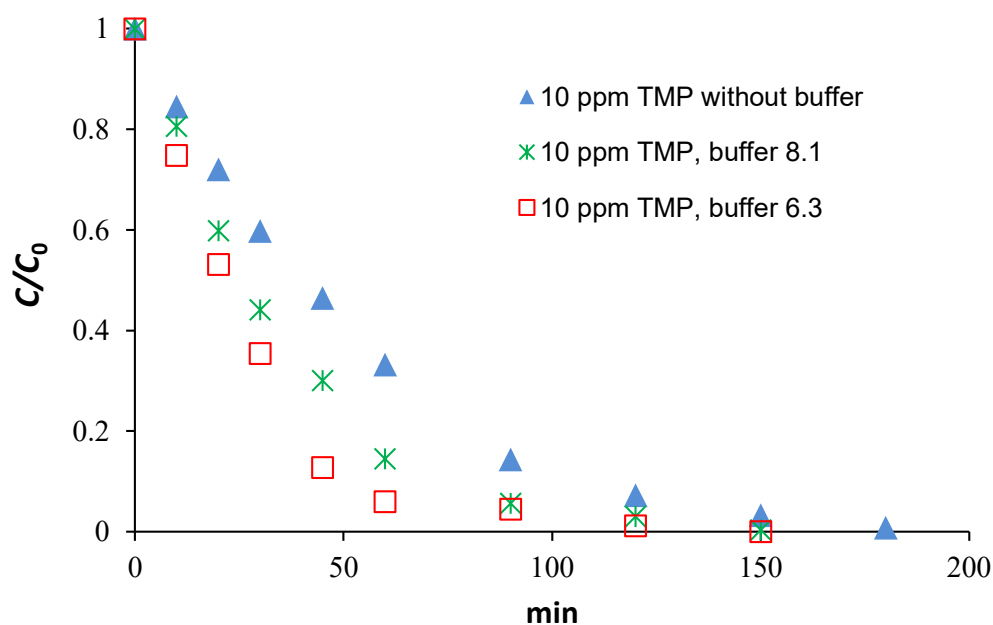
Figure 8. Photocatalytic degradation with and without buffers pH 8.1 and 6.3.

Figure 8 shows that the addition of buffers slightly increases the degradation rate of TMP. The total degradation of TMP can be expected in 2 h of irradiation with the addition of buffer 6.3.

The pH has a significant impact on the photocatalytic degradation process, which is influenced by the ionization state of both the compound and catalyst. The TiO_2 point of the zero charge is 6.25 [45] and plays a crucial role in this process. In buffered TMP solutions, a slightly slower degradation rate was observed at pH 8.1 ($k = 0.0306$ min^{-1}) compared to pH 6.3 ($k = 0.0372$ min^{-1}). The pK_a value of TMP is 7.10 ± 0.02 [46], meaning that at pH < pK_a, TMP will be mostly in its cationic form, while at pH > pK_a, the dominant form of TMP will be neutral. At both investigated pH values, the catalyst surface is negatively charged and TMP is present mostly in its neutral form (90%) at pH 8.1 and in its positively charged form (90%) at pH 6.3 [46], leading to the attraction between the catalyst surface and TMP molecules. The slightly faster degradation at pH 6.3 can be explained by the stronger attraction between cationic TMP and the catalyst surface, compared to neutral TMP at pH 8.1.

In the case of non-buffered TMP solution, the initial pH of 5.59 decreases during oxidation, resulting in a final pH of 3.86, at which TMP is present only in its cationic form. This situation results in both the catalyst surface and TMP being positively charged, leading to repulsion between them and the slower degradation of TMP.

3.4. Energy Consumption

3.4.1. Specific Energy Consumption for the Mineralization of TMP

To determine the energy consumption required for the mineralization of TMP, we calculated the kWh per g of total organic carbon reduction in the solution, as described in [47]. The energy consumption in the experiment came from the simulated solar radiation lamp (with a power of 489 W) and the stirrer (with a power of 10 W). The thermostatic bath, used to maintain a constant temperature of the solution, was not included in the calculation. During the three-hour experiment, the average electric energy consumption was 499 W.

The photocatalytic degradation of TMP without pH adjustment resulted in a TOC reduction of 4.59 mg/L, with a starting TOC value of $TOC_0 = 5.85$ mg/L and a final value of $TOC_{180} = 1.26$ mg/L after three hours.

The energy consumption for this photocatalytic system with a nanostructured photocatalytic film was quite high, resulting in a 3261 kWh/g TOC reduction, which is higher than in the comparative photocatalytic studies (a 5.4–120.0 kWh/g TOC reduction, described in [47], or a 150.34–406.63 kWh/g TOC reduction described in [29]). In this case, the used lamp and reactor dimensions are not optimally matched, as the radiation area of the lamp is larger than the surface area of the reactor and could irradiate at least four such reactors, resulting in unused radiation potential in this experiment. Furthermore, energy consumption optimization was not the primary aim of this study.

It should be noted that the use of a photocatalyst in the form of a film is practically more favorable than in the form of a suspension, as in the comparative studies [29,47]. The degradation of organic matter can be achieved without the need to recycle the photocatalyst, simply by adding a new amount of polluted water to the reactor.

3.4.2. Electrical Energy Per Order (E_{EO}) Analysis

The energy per order of magnitude (E_{EO}) is a figure of merit introduced by Bolton et al. [48] to quantify the electrical efficiency of advanced oxidation processes.

Although the degradation of organic pollutants by AOPs is a complex process involving many elementary reactions, the kinetics can often be approximated by simple zero or first-order expressions [48]. E_{EO} measures the amount of electrical energy (kWh) required to decrease the concentration of a target pollutant in 1 m^3 of water by one order of magnitude (approximately 90%). This performance metric provides a direct comparison of different AOPs regardless of their system types, and lower values indicate higher efficiency [40]. For a batch reactor system, E_{EO} can be calculated using Equation (1) [48],

where t is the time required to reach 90% degradation (min), P is the system's power output (kW), V is the reaction volume (L), and c_i and c_f are the initial and final concentrations of the pollutant (mol/L).

$$E_{\text{EO}} = \frac{P \cdot t \cdot 1000}{V \cdot 60 \cdot \log\left(\frac{c_i}{c_f}\right)} \tag{1}$$

The energy required for the process can be calculated in two ways: (a) by accounting for the electrical consumption of both the lamp and the magnetic stirrer, or (b) by considering only the electrical consumption of the magnetic stirrer, under the assumption that electricity can be obtained from natural solar radiation in real-life scenarios. In case (a), the power meter reading yields p = 499 W (lamp + stirrer). The average reactor volume is V = 0.100 L, and it takes 101.5 min to achieve a 90% reduction. The resulting E_{EO} is 8441.4 kWh/m³. In contrast, for case (b), the power consumption of the magnetic stirrer is only 10 W, with the same volume and time as in case (a). This results in a much lower E_{EO} of 169.2 kWh/m³, when the energy required for the lamp operation is disregarded.

It is worth noting that natural solar radiation can be used to provide the UV-A radiation required for TMP degradation and other organic pollutants. By utilizing solar radiation, the costs associated with generating UV-A radiation can be significantly reduced. This should be considered in future experiments and real-scale reactor design.

To further improve energy efficiency, the size of the reactor should be adjusted to match the radiation source. Additionally, LED bulbs should be used instead of traditional lamps. However, the most important suggestion is to use natural solar radiation whenever possible, as there is no energy cost associated with it. Energy should only be accounted for the stirring process.

4. Conclusions

The degradation and elimination of pharmaceutical compounds from aquatic environments is an urgent environmental challenge that requires sustainable and efficient remediation strategies. In this study, we investigate the photocatalytic degradation of trimethoprim (TMP), a common pharmaceutical, using a nanostructured TiO_2 film on a glass ring under simulated solar irradiation. The results showed that the degradation process is predominantly driven by hydroxyl radicals and positive holes as the primary reactive species, with isopropanol and triethanolamine found to strongly inhibit the photocatalytic degradation of TMP. However, the presence of ammonium oxalate indicates that superoxide radicals do not play a dominant role in the process. The complete degradation of TMP was achieved in less than 3 h under simulated solar radiation, and the specific energy consumption for the mineralization of TMP was calculated to be a 3261 kWh/g TOC reduction. The electrical energy per order (E_{EO}) analysis revealed that using natural solar radiation as a source of UV-A radiation in reactor configurations based on this approach could greatly reduce the cost of pharmaceutical degradation treatment, as evidenced by the results obtained under simulated solar radiation with an irradiation intensity of 33 ± 2 W/m² in the UV-A region. This study provides valuable insights into the photocatalytic degradation mechanism of TMP and highlights the potential of utilizing natural solar radiation to address the challenges of pharmaceutical contamination in aquatic environments.

Institutional Review Board Statement: Not applicable.

Informed Consent Statement: Not applicable.

Data Availability Statement: Not applicable.

Conflicts of Interest: The authors declare no conflict of interest.

References

1. Hernández-Tenorio, R.; González-Juárez, E.; Guzmán-Mar, J.L.; Hinojosa-Reyes, L.; Hernández-Ramírez, A. Review of occurrence of pharmaceuticals worldwide for estimating concentration ranges in aquatic environments at the end of the last decade. *J. Hazard. Mater. Adv.* **2022**, *8*, 100172. [CrossRef]
2. Danfá, S.; Oliveira, C.; Santos, R.; Martins, R.C.; Quina, M.M.J.; Gomes, J. Development of TiO$_2$-Based Photocatalyst Supported on Ceramic Materials for Oxidation of Organic Pollutants in Liquid Phase. *Appl. Sci.* **2022**, *12*, 7941. [CrossRef]
3. Tran, N.H.; Reinhard, M.; Gin, Y.-H.K. Occurrence and fate of emerging contaminants in municipal wastewater treatment plants from different geographical regions—A review. *Water Res.* **2018**, *133*, 182–207. [CrossRef] [PubMed]
4. Luo, Y.; Guo, W.; Ngo, H.H.; Nghiem, L.D.; Hai, F.I.; Zhang, J.; Liang, S.I.; Wang, X.C. A review on the occurrence of micropollutants in the aquatic environment and their fate and removal during wastewater treatment. *Sci. Total Environ.* **2014**, *473*, 619–641. [CrossRef] [PubMed]
5. Gros, M.; Petrović, M.; Ginebreda, A.; Barcelo, D. Removal of pharmaceuticals during wastewater treatment and environmental risk assessment using hazard indexes. *Environ. Int.* **2010**, *36*, 15–26. [CrossRef]
6. Falas, P.; Wick, A.; Castronovo, S.; Habermacher, J.; Ternes, T.A.; Joss, A. Tracing the limits of organic micropollutant removal in biological wastewater treatment. *Water Res.* **2016**, *95*, 240–249. [CrossRef]
7. Aktar, W.; Sengupta, D.; Chowdhury, A. Impact of pesticides use in agriculture: Their benefits and hazards. *Interdiscip. Toxicol.* **2009**, *2*, 1–12. [CrossRef]
8. Li, W.C. Occurrence, sources, and fate of pharmaceuticals in aquatic environment and soil. *Environ. Pollut.* **2014**, *187*, 193–201. [CrossRef] [PubMed]
9. Petrović, M.; Gonzales, S.; Barcelo, D. Analysis and removal of emerging contaminants in wastewater and drinking water. *TrAC Trends Anal. Chem.* **2003**, *10*, 685–696. [CrossRef]
10. Biošić, M.; Babić, S. Trimethoprim elimination by biotic and abiotic processes. *Fresenius Environ. Bul.* **2020**, *29*, 7972–7979.
11. Le, T.X.; Munekage, Y.; Kato, S. Antibiotic resistance in bacteria from shrimp farming in mangrove areas. *Sci. Total Environ.* **2005**, *349*, 95–105. [CrossRef]
12. Watson, M.; Liu, J.-W.; Ollis, D. Directed evolution of trimethoprim resistance in Escherichia coli. *FEBS J.* **2007**, *274*, 2661–2671. [CrossRef]
13. Amarasiri, M.; Sano, D.; Suzuki, S. Understanding human health risks caused by antibiotic resistant bacteria (ARB) and antibiotic resistance genes (ARG) in water environments: Current knowledge and questions to be answered. *Crit. Rev. Environ. Sci. Technol.* **2020**, *50*, 2016–2059. [CrossRef]
14. Yilmaz, G.; Kaya, Y.; Vergili, I.; Gönder, Z.B.; Özhan, G.; Ozbek Celik, B.; Altinkum, S.M.; Bagdatli, Y.; Boergers, A.; Tuerk, J. Characterization and toxicity of hospital wastewaters in Turkey. *Environ. Monit. Assess.* **2017**, *189*, 1–19.
15. Mpatani, F.M.; Aryee, A.A.; Kani, A.N.; Han, R.; Li, Z.; Dovi, E.; Qu, L. A review of treatment techniques applied for selective removal of emerging pollutant-trimethoprim from aqueous systems. *J. Clean. Prod.* **2021**, *308*, 127359. [CrossRef]
16. Alharbi, S.K.; Kang, J.; Nghiem, L.D.; van de Merwe, J.P.; Leusch, F.D.L.; Price, E.E. Photolysis and UV/H$_2$O$_2$ of diclofenac, sulfamethoxazole, carbamazepine, and trimethoprim: Identification of their major degradation products by ESI–LC–MS and assessment of the toxicity of reaction mixtures. *Process Saf. Environ. Prot.* **2017**, *112 Pt B*, 222–234. [CrossRef]
17. Ryan, C.C.H.; Tan, D.T.; Arnold, W.A. Direct and indirect photolysis of sulfame thoxazole and trimethoprim in wastewater treatment plant effluent. *Water Res.* **2012**, *45*, 1280–1286. [CrossRef]
18. Adil, S.; Maryam, B.; Kim, E.-J.; Dulova, N. Individual and simultaneous degradation of sulfamethoxazole and trimethoprim by ozone, ozone/hydrogen peroxide and ozone/persulfate processes: A comparative study. *Environ. Res.* **2020**, *189*, 109889. [CrossRef] [PubMed]

19. Abellán, M.N.; Giménez, J.; Esplugas, S. Photocatalytic degradation of antibiotics: The case of sulfamethoxazole and trimethoprim. *Catal. Today* **2009**, *144*, 131–136. [CrossRef]

20. Radjenović, J.; Petrović, M.; Venture, F.; Barcelo, D. Rejection of pharmaceuticals in nanofiltration and reverse osmosis membrane drinking water treatment. *Water Res.* **2008**, *42*, 3601–3610. [CrossRef]

21. Zhang, G.; Yu, Y.; Tu, Y.; Liu, Y.; Huang, J.; Yin, X.; Feng, Y. Preparation of reusable UHMWPE/TiO2 photocatalytic microporous membrane reactors for efficient degradation of organic pollutants in water. *Sep. Purif. Technol.* **2023**, *305*, 122515. [CrossRef]

22. Arvaniti, O.S.; Frontistis, Z.; Nika, M.C.; Aalizadeh, R.; Thomaidis, N.S.; Mantzavinos, D. Sonochemical degradation of trimethoprim in water matrices: Effect of operating conditions, identification of transformation products and toxicity assessment. *Ultrason. Sonochem.* **2020**, *67*, 105139. [CrossRef]

23. Liu, R.; Yu, H.; Hou, X.; Liu, X.; Bi, E.; Wang, W.; Li, M. Typical Sulfonamide Antibiotics Removal by Biochar-Amended River Coarse Sand during Groundwater Recharge. *Int. J. Environ. Res. Public Health* **2022**, *19*, 16957. [CrossRef]

24. Juengchareonpoon, K.; Wanichpongpan, P.; Boonamnuayvitaya, V. Trimethoprim adsorption using graphene oxide-carboxymethylcellulose film coated on polyethylene terephthalate as a supporter. *Chem. Eng. Process. Process Intensif.* **2021**, *169*, 108641. [CrossRef]

25. Mohammadzadeh, M.; Leiviskä, T. Iron-modified peat and magnetite-pine bark biosorbents for levofloxacin and trimethoprim removal from synthetic water and various pharmaceuticals from real wastewater. *Ind. Crops Prod.* **2023**, *195*, 116491. [CrossRef]

26. Lu, H.; Wang, J.; Stoller, M.; Wang, T.; Bao, Y.; Hao, H. An Overview of Nanomaterials for Water and Wastewater Treatment. *Adv. Mater. Sci. Eng.* **2016**, *2016*, 4964828. [CrossRef]

27. Ljubas, D.; Franzreb, M.; Bruun Hansen, H.C.; Weidler, P.G. Magnetizing of nano-materials on example of Degussa's P-25 TiO2 photocatalyst: Synthesis of magnetic aggregates, characterization and possible use. *Sep. Purif. Technol.* **2014**, *136*, 274–285. [CrossRef]

28. Kocijan, M.; Ćurković, L.; Ljubas, D.; Mužina, K.; Bačić, I.; Radošević, T.; Podlogar, M.; Bdikin, I.; Otero-Irurueta, G.; Hortigüela, M.J.; et al. Graphene-based TiO2 nanocomposite for photocatalytic degradation of dyes in aqueous solution under solar-like radiation. *Appl. Sci.* **2021**, *11*, 3966. [CrossRef]

29. Babić, S.; Zrnčić, M.; Ljubas, D.; Ćurković, L.; Škorić, I. Photolytic and thin TiO2 film assisted photocatalytic degradation of sulfamethazine in aqueous solution. *Environ. Sci. Pollut. Res.* **2015**, *22*, 11372–11386. [CrossRef] [PubMed]

30. Araújo, A.; Soares, O.S.G.P.; Orge, C.A.; Gonçalves, A.G.; Rombi, E.; Cutrufello, M.G.; Fonseca, A.M.; Pereira, M.F.R.; Neves, I.C. Metal-zeolite catalysts for the removal of pharmaceutical pollutants in water by catalytic ozonation. *Environ. Chem. Eng.* **2021**, *9*, 106458. [CrossRef]

31. Hoffmann, M.R.; Martin, S.T.; Choi, W.; Bahnemann, D.W. Environmental applications of semiconductor photocatalysis. *Chem. Rev.* **1995**, *95*, 69–96. [CrossRef]

32. Linsebigler, A.L.; Lu, G.; Yates, J.T., Jr. Photocatalysis on TiO2 surfaces: Principles, Mechanisms and selected results. *Chem. Rev.* **1995**, *95*, 735–758. [CrossRef]

33. Gaya, U.I.; Abdullah, A.H. Heterogeneous photocatalytic degradation of organic contaminants over titanium dioxide: A review of fundamentals, progress and problems. *J. Photochem. Photobiol. C Photochem.* **2008**, *9*, 1–12. [CrossRef]

34. Feng, Y.; Rijnaarts, H.H.M.; Yntema, D.; Gong, Z.; Dionysiou, D.D.; Cao, Z.; Miao, S.; Chen, Y.; Ye, Y.; Wang, Y. Applications of anodized TiO2 nanotube arrays on the removal of aqueous contaminants of emerging concern: A review. *Water Res.* **2020**, *186*, 116327. [CrossRef]

35. Pozzo, R.L.; Baltanas, M.A.; Cassano, A.E. Supported titanium oxide as photocatalyst in water decontamination: State of the art. *Catal. Today* **1997**, *39*, 219–231. [CrossRef]

36. Pozzo, R.L.; Baltanas, M.A.; Cassano, A.E. Towards a precise assessment of the performance of supported photocatalysts for water detoxification processes. *Catal. Today* **1999**, *54*, 43–157. [CrossRef]

37. Rueda-Márquez, J.J.; Palacios-Villarreal, C.; Manzano, M.; Blanco, E.; Ramírez del Solar, M.; Levchuk, I. Photocatalytic degradation of pharmaceutically active compounds (PhACs) in urban wastewater treatment plants effluents under controlled and natural solar irradiation using immobilized TiO2. *Sol. Energy* **2020**, *208*, 480–492. [CrossRef]

38. Matoh, L.; Žener, B.; Kovačić, M.; Kušić, H.; Arčon, I.; Levstek, M.; Lavrenčič Štangar, U. Photocatalytic sol-gel/P25 TiO2 coatings for water treatment: Degradation of 7 selected pharmaceuticals. *Ceram. Int.* **2022**; *in press*. [CrossRef]

39. Šegota, S.; Ćurković, L.; Ljubas, D.; Svetličić, V.; Fiamengo Houra, I.; Tomašić, N. Synthesis, characterization and photocatalytic properties of sol–gel TiO2 films. *Ceram. Int.* **2011**, *37*, 1153–1160. [CrossRef]

40. Ćurković, L.; Ljubas, D.; Šegota, S.; Bačić, I. Photocatalytic degradation of Lissamine Green B dye by using nanostructured sol-gel TiO2 films. *J. Alloys Compd.* **2014**, *604*, 309–316. [CrossRef]

41. Samy, M.; Ibrahim, M.G.; Gar Alalm, M.; Fujii, M.; Ookawara, S.; Ohno, T. Photocatalytic degradation of trimethoprim using S-TiO2 and Ru/WO3/ZrO2 immobilized on reusable fixed plates. *J. Water Process. Eng.* **2020**, *33*, 101023. [CrossRef]

42. Sarafraz, M.; Sadeghi, M.; Yazdanbakhsh, A.; Amini, M.M.; Sadani, M.; Eslami, A. Enhanced photocatalytic degradation of ciprofloxacin by black Ti3+/N-TiO2 under visible LED light irradiation: Kinetic, energy consumption, degradation pathway, and toxicity assessment. *Process Saf. Environ. Prot.* **2020**, *137*, 261–272. [CrossRef]

43. Sirtori, C.; Aguera, A.; Gernjak, W.; Malato, S. Effect of water-matrix composition on Trimethoprim solar photodegradation kinetics and pathways. *Water Res.* **2010**, *44*, 2735–2744. [CrossRef]

44. Bekbolet, M.; Serif Suphandag, A.; Senem Uyguner, C. An investigation of the photocatalytic efficiencies of TiO$_2$ powders on the decolourisation of humic acids. *J. Photochem. Photobiol. A Chem.* **2020**, *148*, 121–128. [CrossRef]

45. Gilbert, E.; von Hodenberg, S. Einfluss aliphatischer Dicarbonsäuren auf die fotokatalytische Elimination von Naphtalin-1,5-disulfonsäure mit Titandioxid. *Vom Wasser* **2001**, *97*, 135–144.

46. Zrnčić, M.; Babić, S.; Mutavdžić Pavlović, D. Determination of thermodynamic pK_a values of pharmaceuticals from five different groups using capillary electrophoresis. *J. Sep. Sci.* **2015**, *38*, 1232–1239. [CrossRef]

47. Kopf, P.; Gilbert, E.; Eberle, S.H. TiO$_2$ photocatalytic oxidation of monochloroacetic acid and pyridine: Influence of ozone. *J. Photochem. Photobiol. A Chem.* **2000**, *136*, 163–168. [CrossRef]

48. Bolton, J.R.; Bircher, K.G.; Tumas, W.; Tolman, C.A. Figures-of-merit for the technical development and application of advanced oxidation technologies for both electric- and solar-driven systems (IUPAC Technical Report). *Pure Appl. Chem.* **2001**, *73*, 627–637. [CrossRef]